Nrf2 links epidermal barrier function with antioxidant defense

*Matthias Schäfer[1]**, Hany Farwanah[2], Ann-Helen Willrodt[1], Aaron J. Huebner[3], Konrad Sandhoff[2], Dennis Roop[3], Daniel Hohl[4], Wilhelm Bloch[5], Sabine Werner[1]**

Keywords: barrier function; inflammation; Nrf2; oxidative stress; skin

DOI 10.1002/emmm.201200219

Received October 01, 2011
Revised January 17, 2012
Accepted January 20, 2012

→See accompanying article
http://dx.doi.org/10.1002/emmm.201200223

The skin provides an efficient permeability barrier and protects from microbial invasion and oxidative stress. Here, we show that these essential functions are linked through the Nrf2 transcription factor. To test the hypothesis that activation of Nrf2 provides skin protection under stress conditions, we determined the consequences of pharmacological or genetic activation of Nrf2 in keratinocytes. Surprisingly, mice with enhanced Nrf2 activity in keratinocytes developed epidermal thickening, hyperkeratosis and inflammation resembling lamellar ichthyosis. This resulted from upregulation of the cornified envelope proteins small proline-rich proteins (Sprr) 2d and 2h and of secretory leukocyte peptidase inhibitor (Slpi), which we identified as novel Nrf2 targets in keratinocytes. Since Sprrs are potent scavengers of reactive oxygen species and since Slpi has antimicrobial activities, their upregulation contributes to Nrf2's protective function. However, it also caused corneocyte fragility and impaired desquamation, followed by alterations in the epidermal lipid barrier, inflammation and overexpression of mitogens that induced keratinocyte hyperproliferation. These results identify an unexpected role of Nrf2 in epidermal barrier function, which needs to be considered for pharmacological use of Nrf2 activators.

INTRODUCTION

Reactive oxygen species (ROS) are highly aggressive molecules that are produced in various cellular reactions, for example in the respiratory chain. ROS levels are strongly elevated in response to different insults, such as exposure to xenobiotics or UV irradiation. While low levels of ROS are required for efficient intracellular signalling, high levels are deleterious, as they damage cellular macromolecules including DNA. ROS-induced cell damage is involved in the pathogenesis of major human diseases including cancer and neurodegenerative diseases (de Vries et al, 2008; Liou & Storz, 2010; Perez-Matute et al, 2009).

To cope with ROS, cells have evolved antioxidant defense mechanisms. A central player is nuclear factor erythroid derived 2, like 2 (Nrf2), which regulates the expression of numerous detoxifying enzymes and antioxidant proteins and is highly conserved throughout evolution (Sykiotis & Bohmann, 2010). *Nrf2* knockout (ko) mice show a reduction in the basal and inducible expression of cytoprotective genes, and are more susceptible to the toxicity of ROS-inducing agents and electrophiles (Copple et al, 2008).

Vice versa, Nrf2 activation efficiently protected cells from ROS damage *in vitro* and *in vivo*. Most importantly, a variety of Nrf2-activating substances showed a potent chemopreventive and anti-inflammatory function in animal models of cancer (Kundu

(1) Department of Biology, Institute of Cell Biology, ETH Zurich, Zurich, Switzerland
(2) LIMES, Membrane Biology & Lipid Biochemistry Unit, c/o Kekulé-Institute for Organic Chemistry and Biochemistry, University of Bonn, Bonn, Germany
(3) Department of Dermatology, School of Medicine, University of Colorado Denver, Aurora, CO, USA
(4) Department of Dermatology, University Hospital of Lausanne (CHUV), Lausanne, Switzerland
(5) Department of Molecular and Cellular Sport Medicine, German Sport University Cologne, Cologne, Germany
Corresponding author: Tel: +41 44 633 3941; Fax: +41 44 633 1174; E-mail: sabine.werner@cell.biol.ethz.ch
Corresponding author: Tel: +41 44 633 3406; Fax: +41 44 633 1174; E-mail: matthias.schaefer@cell.biol.ethz.ch

& Surh, 2010; Kwak & Kensler, 2010; Ramos-Gomez et al, 2001; Xu et al, 2006). Clinical trials confirmed a chemopreventive function of the Nrf2 activators sulforaphane and triterpenoids in humans (Liby et al, 2007; Yanaka et al, 2009). Promising results with Nrf2 activators have also been obtained in animal models of neurodegenerative diseases (de Vries et al, 2008). Furthermore, diet restriction-induced longevity in *Caenorhabditis elegans* (*C. elegans*) requires the Nrf2 homologue Skn-1 (Bishop & Guarente, 2007).

In spite of these positive and encouraging results, Nrf2 activation may also have adverse effects. Constitutive activation of Nrf2 through genetic or epigenetic mechanisms or upregulation of Nrf2 expression by oncogenes have been identified in various tumours, which are associated with enhanced cell proliferation, reduced apoptosis and enhanced chemoresistance of tumour cells (Denicola et al, 2011; Hayes & McMahon, 2009). It is therefore essential to examine the consequences of pharmacological use of Nrf2 activators and their effect on tissue homeostasis before they are brought into the clinic.

The skin, which serves as a protective barrier against the environment, is frequently challenged by harmful insults that cause oxidative stress. Pharmacological activation of Nrf2 in the skin protected against chemically- and UV-induced carcinogenesis (Dinkova-Kostova et al, 2006; Xu et al, 2006). Furthermore, transgenic mice expressing a constitutively active Nrf2 mutant in keratinocytes were remarkably resistant to UVB-induced ROS damage (Schäfer et al, 2010). As a result of these studies several patents for the use of Nrf2 activators as skin protecting agents were filed, for example for sulforaphane [publication number KR20080045083 (A)] or oltipraz [publication number KR20020075954 (A)]. It needs to be considered, however, that mice lacking the Nrf2 antagonist Keap1 show hyperkeratosis in the skin (Taguchi et al, 2010; Wakabayashi et al, 2003) and that Nrf2-activating mutations have been identified in cutaneous squamous cell carcinomas (Kim et al, 2010). Thus, activation of Nrf2 in the skin may have harmful effects.

Here, we show that Nrf2 links antioxidant defense mechanisms in the epidermis with control of the permeability barrier and antimicrobial defense. While limited activation of these mechanisms is beneficial, prolonged activation of Nrf2 in the epidermis caused corneocyte fragility and impaired desquamation, resulting in the development of an ichthyosis-like skin disease. These findings unravelled an unexpected role of Nrf2 in skin homeostasis and disease that goes well beyond its well-characterized antioxidant function.

RESULTS

Genetic activation of Nrf2-mediated gene expression in keratinocytes disrupts skin homeostasis

To specifically activate Nrf2 in keratinocytes *in vivo* and to exclude potential Nrf2-independent effects of pharmacological Nrf2 activators, we generated transgenic mice expressing a constitutively active Nrf2 mutant (caNrf2) in keratinocytes. We previously reported on the characterization of this mutant and generation of mice expressing caNrf2 under control of a β-actin promoter (Schäfer et al, 2010) using a construct containing the *caNrf2* cDNA preceded by a floxed stop cassette. Crossing of β-actin-caNrf2 mice with transgenic mice expressing Cre recombinase under control of the keratin 5 (*K5*) promoter allowed Cre-induced activation of Nrf2-mediated gene expression in keratinocytes (Schäfer et al, 2010).

To further characterize the phenotype of these mice and to identify a possible dose-dependency, we generated mice expressing the same transgene but with a *CMV* enhancer upstream of the *β-actin* promoter (Sawicki et al, 1998; Fig 1A). These mice were crossed with K5-cre mice and the progeny was named K5cre-CMVcaNrf2 mice (Fig 1A). RNase protection assay (RPA) using RNAs from skin of mice hemizygous for the *caNrf2* transgene revealed an approximately fourfold higher expression of *caNrf2* in K5cre-CMVcaNrf2 compared to K5cre-caNrf2 mice (Fig 1B). Consequently, a higher expression of the Nrf2 target genes NAD(P)H dehydrogenase, chinone 1 (*Nqo1*), glutamate cysteine ligase catalytic subunit (*Gclc*) and modifier subunit (*Gclm*) and sulphiredoxin (*Srxn*) was observed (Fig 1C).

K5cre-CMVcaNrf2 mice displayed reduced body size and weight as well as hair loss (Fig S1A of Supporting information and Fig 1D). Their skin appeared dry and there was considerable scaling. Histological analysis revealed a thickened viable epidermis (acanthosis) and stratum corneum (SC) (hyperkeratosis), enlarged sebaceous glands and hair follicle abnormalities (Fig 1E). Hyperkeratosis was also described in *Keap1*-deficient mice, which die, however, 3 weeks after birth from malnutrition due to hyperkeratosis in the esophagus (Wakabayashi et al, 2003). By contrast, K5cre-CMVcaNrf2 mice are viable and do not show hyperkeratosis in the esophagus, oral epithelium, tongue and forestomach.

Pharmacological Nrf2 activators cause phenotypic abnormalities resembling caNrf2 transgenic mice

To determine if activation of endogenous Nrf2 causes similar abnormalities, newborn wild-type (WT) mice (FVB/N/C57BL/6 mixed background) were topically treated with the Nrf2 activators sulforaphane or *tert*-butyl hydrochinone (*t*BHQ) or with vehicle. Indeed, treatment with the Nrf2 activators also caused hyperkeratosis, acanthosis and sebaceous gland enlargement (Fig 2A). A strong increase in the expression of *Nqo1*, *Gclc*, *Gclm* and glutathione S-transferase alpha 3 (*Gsta3*) revealed efficient Nrf2 activation under these conditions (Fig 2B).

Morphometrical analysis confirmed a significant increase in the thickness of the viable epidermis in sulforaphane- and *t*BHQ-treated mice (Fig 2C), but only a mild increase in vehicle-treated animals. The stronger effect of *t*BHQ compared to sulforaphane correlates with the extent of Nrf2 target gene activation (Fig 2B). Most importantly, the *t*BHQ-induced increase in epidermal thickness was not observed in *Nrf2* ko mice (C57BL/6 background), whereas it was reproduced in their wt littermates (Fig 2D). These findings strongly suggest that the epidermal abnormalities observed in caNrf2 transgenic mice indeed result from activation of Nrf2-mediated gene expression. Therefore, caNrf2 transgenic mice represent a valuable model to study the consequences of Nrf2 activation in the skin.

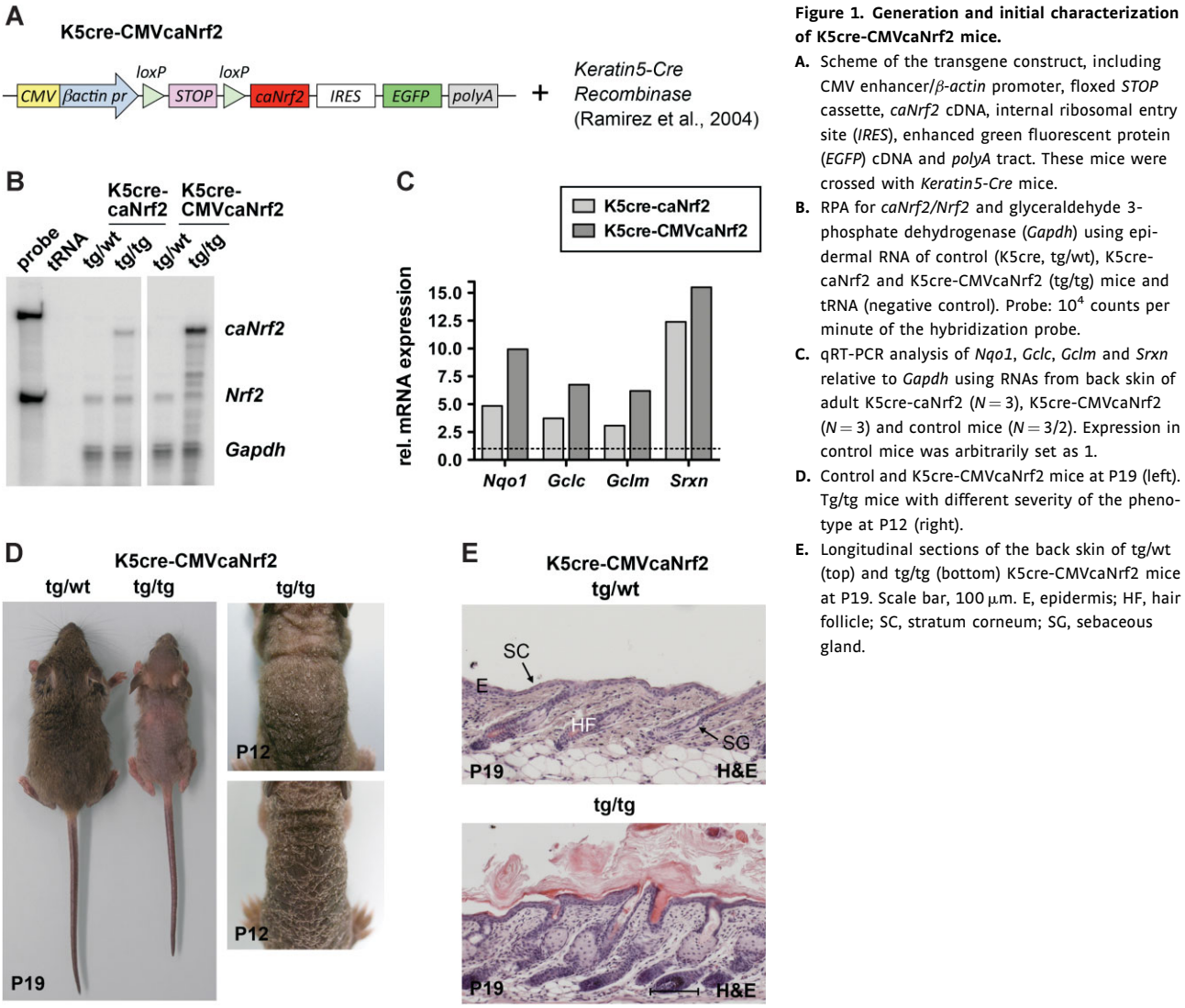

Figure 1. Generation and initial characterization of K5cre-CMVcaNrf2 mice.

A. Scheme of the transgene construct, including CMV enhancer/*β-actin* promoter, floxed *STOP* cassette, *caNrf2* cDNA, internal ribosomal entry site (*IRES*), enhanced green fluorescent protein (*EGFP*) cDNA and *polyA* tract. These mice were crossed with *Keratin5-Cre* mice.

B. RPA for *caNrf2/Nrf2* and glyceraldehyde 3-phosphate dehydrogenase (*Gapdh*) using epidermal RNA of control (K5cre, tg/wt), K5cre-caNrf2 and K5cre-CMVcaNrf2 (tg/tg) mice and tRNA (negative control). Probe: 10^4 counts per minute of the hybridization probe.

C. qRT-PCR analysis of *Nqo1*, *Gclc*, *Gclm* and *Srxn* relative to *Gapdh* using RNAs from back skin of adult K5cre-caNrf2 ($N = 3$), K5cre-CMVcaNrf2 ($N = 3$) and control mice ($N = 3/2$). Expression in control mice was arbitrarily set as 1.

D. Control and K5cre-CMVcaNrf2 mice at P19 (left). Tg/tg mice with different severity of the phenotype at P12 (right).

E. Longitudinal sections of the back skin of tg/wt (top) and tg/tg (bottom) K5cre-CMVcaNrf2 mice at P19. Scale bar, 100 μm. E, epidermis; HF, hair follicle; SC, stratum corneum; SG, sebaceous gland.

Activation of Nrf2 causes an ichthyosis-like phenotype

The epidermal abnormalities observed in mice after Nrf2 activation are remarkably reminiscent to those seen in the heterogeneous group of ichthyosis diseases, in particular in lamellar ichthyosis (Hohl & Williams, 2011). Therefore, we determined if there are similarities in the underlying pathomechanisms. We focused on the epidermal phenotype in K5cre-CMVcaNrf2 mice, whereas, sebaceous gland and hair follicle abnormalities will be characterized in a separate study.

The epidermal phenotype of K5cre-CMVcaNrf2 mice developed in the first postnatal weeks and was most severe in mice at the age of 1–3 months. However, the phenotype frequently ameliorated upon aging as shown for mice at the age of 6 months (Fig 3A). This time course correlates with a higher expression of the caNrf2 transgene in adult compared to newborn mice and with a decline of expression in aged mice (Supporting information Fig S1B).

Immunostaining of skin sections with antibodies against epidermal differentiation markers was performed at P32, when hairs of K5cre-CMVcaNrf2 and control mice were both in anagen. Loricrin (Lor), involucrin (Inv), K10 and K14 showed an extended expression in the interfollicular epidermis of K5cre-CMVcaNrf2 mice, but were still normally distributed (Fig 3B). Interfollicular expression of K6 was not observed (Fig 3B). Thus, caNrf2 expression does not generally interfere with the normal epidermal differentiation program.

Similar to the situation seen in ichthyosis (Elias et al, 2008), basal keratinocytes were strongly hyperproliferative in K5cre-CMVcaNrf2 transgenic mice at P32 (Fig 3C). Consistent with the milder acanthosis in older animals (Fig 3A), the rate of proliferation declined in 6-month-old mice (Fig 3C). The hyperproliferation observed *in vivo* is not a cell-autonomous effect of Nrf2 activation as demonstrated by the normal proliferation rate of cultured keratinocytes (Fig 3D). Apoptotic cells were rare in the epidermis of control mice and were even

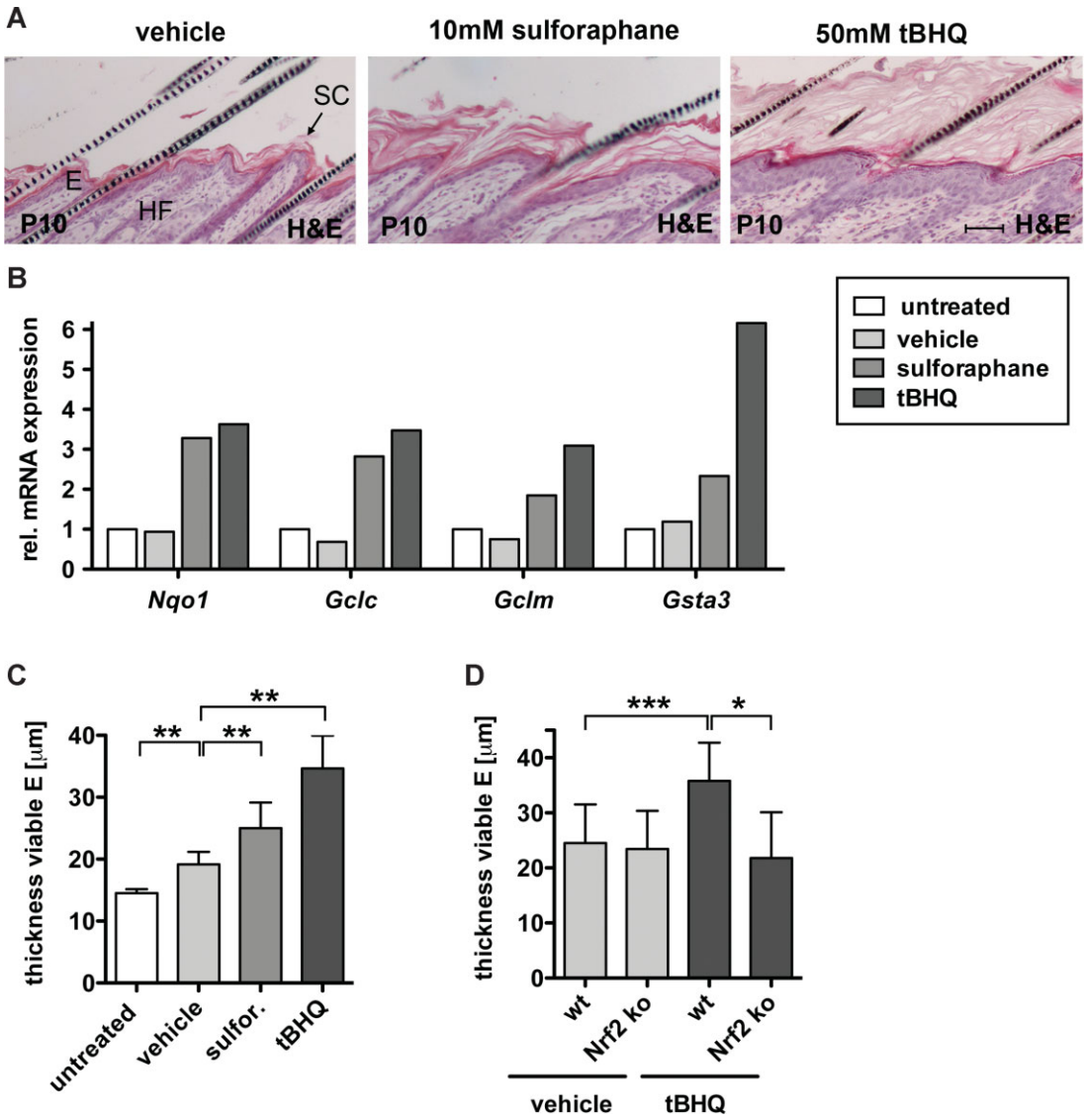

Figure 2. Pharmacological activation of Nrf2 in the skin phenocopies genetic activation.

A. H&E staining of longitudinal skin sections from mice topically treated with vehicle, 10 mM sulforaphane (sulfor) or 50 mM *t*BHQ showing hyperkeratosis and acanthosis in sulforaphane and *t*BHQ treated mice. Scale bar, 50 μm. E, epidermis; HF, hair follicle; SC, stratum corneum.

B. qRT-PCR analysis of *Nqo1*, *Gclc*, *Gclm* and *Gsta3* relative to *Gapdh* using RNAs from back skin of the differently treated mice (control, $N = 3$; vehicle, $N = 3$; sulforaphane, $N = 3$; *t*BHQ, $N = 3$). Expression levels in untreated mice were arbitrary set to 1 (dashed line).

C. Thickness of the viable epidermis in untreated ($N = 10$), vehicle ($N = 6$, $^{**}p = 0.0022$), sulforaphane ($N = 6$, $^{**}p = 0.0022$) or *t*BHQ ($N = 6$, $^{**}p = 0.0012$) treated WT mice.

D. Thickness of the viable epidermis in WT and *Nrf2* ko mice treated with vehicle or *t*BHQ. Epidermal thickness increased in WT mice ($N = 15/17$, $^{***}p = 0.0003$), but not in *Nrf2* ko mice ($N = 17/5$, $^{**}p = 0.0118$).

further reduced in transgenic mice (Fig 3E). Thus, the acanthosis in K5cre-CMVcaNrf2 transgenic mice results predominantly from enhanced keratinocyte proliferation.

K5cre-CMVcaNrf2 mice have a disturbed epidermal barrier

We next determined if the acanthosis and hyperkeratosis result from induction of compensatory mechanisms due to disturbance of the epidermal barrier as seen in patients with ichthyosis (Proksch et al, 2008). Therefore, we measured the transepidermal water loss (TEWL) on the back skin to determine if the inside-out barrier function is affected. No difference was seen between control and transgenic mice at P2.5 (Fig 3F), but TEWL was significantly increased in transgenic mice at P10 (2x), P32 (2.5x) and 6 months (6m) (2x; Fig 3F). This time course correlates with the establishment of the phenotype in the first postnatal weeks and the milder phenotype in aged mice.

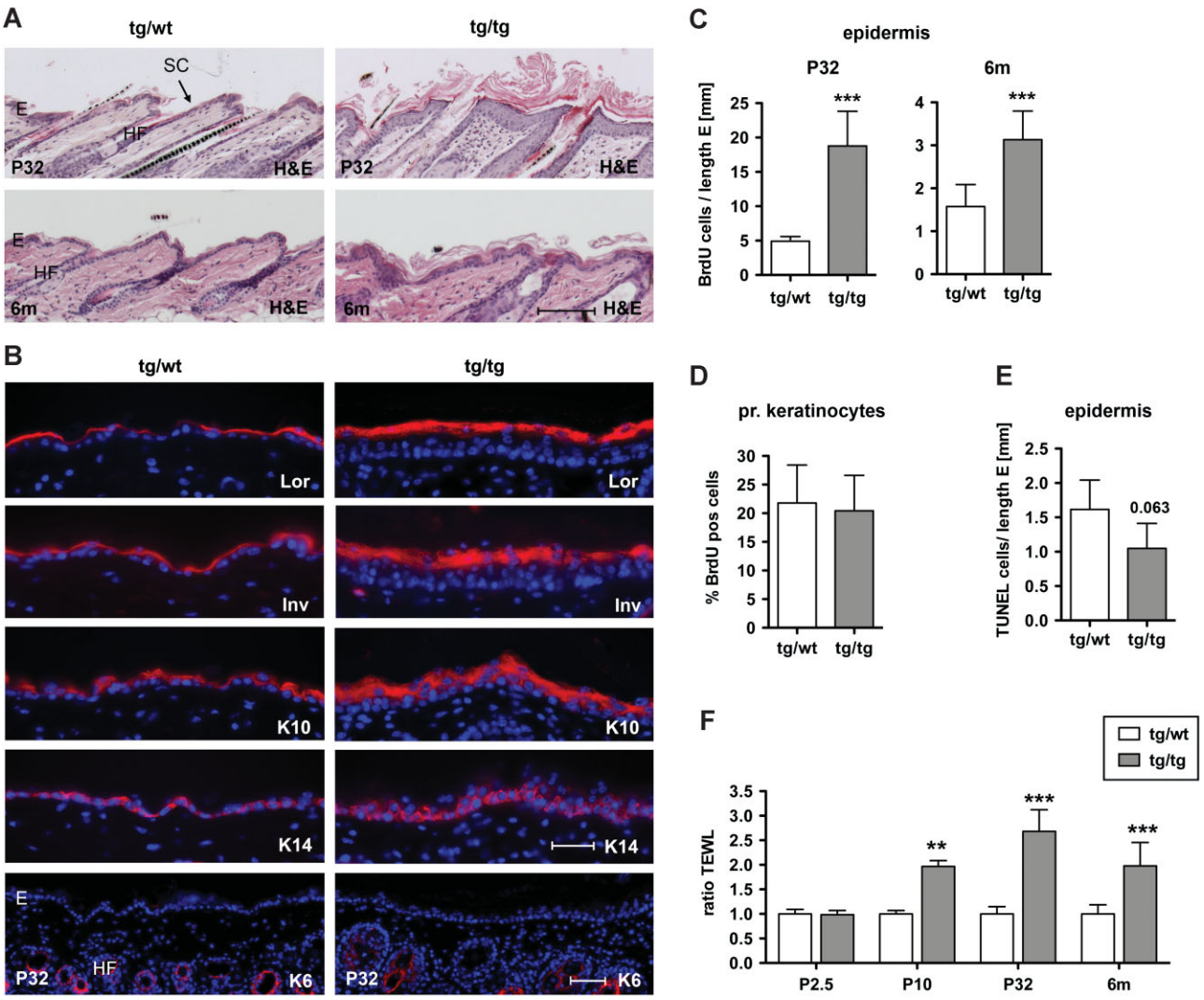

Figure 3. Hyperproliferation, impaired barrier function and inflammation in K5cre-CMVcaNrf2 mice.

A. H&E staining of P32 (upper panel) and 6 months (lower panel) K5cre-CMVcaNrf2 and control skin sections. Scale bar, 100 μm.

B. Immunofluorescence analysis of Lor, Inv, K10, K14 and K6 (red), counterstained with Hoechst (blue). Scale bars, Lor, Inv, K10 and K14, 30 μm; K6, 50 μm. E, epidermis; HF, hair follicle; SC, stratum corneum.

C. BrdU positive cells per length epidermis at P32 ($^{***}p = 0.0004$) and 6 months of age ($^{***}p = 0.0004$).

D. Percentage of BrdU positive subconfluent primary keratinocytes from tg/wt and tg/tg mice.

E. TUNEL positive cells per length epidermis at P32 ($N = 4/5$, $p = 0.063$).

F. TEWL at P2.5 ($N = 4/2$), P10 ($N = 8/4$, $^{**}p = 0.0016$), P32 ($N = 10/6$, $^{***}p = 0.0002$) and 6 months ($N = 11/12$, $^{***}p < 0.0001$).

The increased TEWL provides a likely explanation for the skin dryness and may underlie at least in part the reduction in body weight (see Fig 1D and Fig S1A of Supporting information).

A defect in the epidermal barrier frequently initiates an inflammatory response (Elias, 2010). Indeed, immunofluorescence and histochemical staining of P32 skin revealed an increase in the number of dermal T cells ($CD3^+$), mast cells (toluidine blue staining) and neutrophils ($Ly\text{-}6G^+$) in K5cre-CMVcaNrf2 mice, while numbers of macrophages (macrophage specific lectin) and epidermal T cells ($CD3^+$) were normal (Fig 4A and Fig S1C and D of Supporting information). This correlated with enhanced mRNA levels of the pro-inflammatory cytokines interferon-γ (*Ifnγ*), interleukin-1β (*Il1β*), *Il6* and tumour necrosis factor-α (*Tnfα*) at P32, while expression of thymic stromal lymphopoietin (*Tslp*), a driver of allergic asthma (Demehri et al, 2009), was even slightly downregulated (Fig 4B). Since there was no inflammatory infiltrate and only an increase in *Il1β* expression at P2.5 (Fig 4B), the inflammation is most likely a consequence of the epidermal barrier defect, which develops in the first days of postnatal development as shown by TEWL (see Fig 3F).

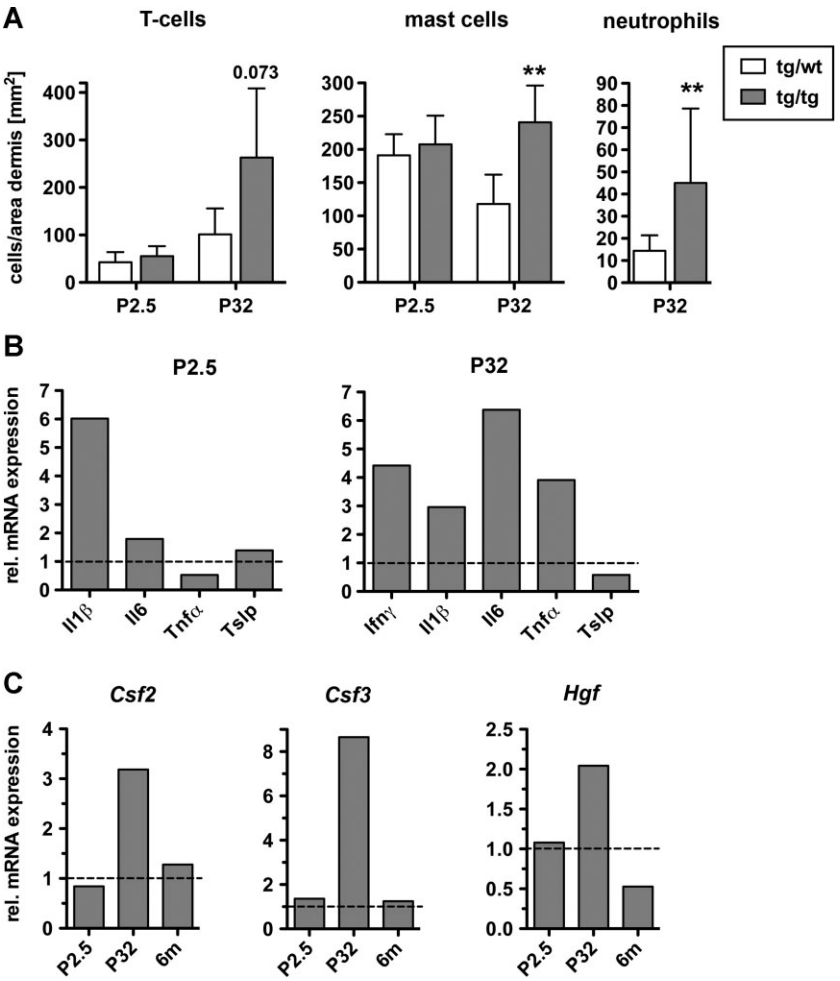

Figure 4. Inflammation in K5cre-CMVcaNrf2 mice.

A. Number of CD3 positive T cells, toluidine blue positive mast cells and Ly-6G positive neutrophils per area dermis at P2.5 and P32 (CD3: $N = 5/4$ for P2.5 mice, $N = 7/5$, $p = 0.0732$ for P32 mice; toluidine blue: $N = 6/5$ for P2.5 mice, $N = 8/6$, $^{**}p = 0.0013$ for P32 mice; Ly-6G: $N = 8/6$, $^{**}p = 0.0047$ for P32 mice).

B. qRT-PCR of *Ifnγ*, *Il1β*, *Il6* and *Tnfα* and *Tslp* relative to *Gapdh* using RNAs from P2.5 (left, $N = 2/3$) and P32 (right, $N = 3$) tg/wt and tg/tg mice. At P2.5 *Ifnγ* RNA was not detectable.

C. qRT-PCR of *Csf2*, *Csf3* and *Hgf* relative to *Gapdh* using RNAs from the skin of tg/wt and tg/tg K5cre-CMVcaNrf2 mice at P2.5 ($N = 2/3$), P32 ($N = 3$) and 6 months ($N = 3$). Expression levels of control mice were arbitrarily set to 1 (dashed lines).

The progressive inflammation also provides a likely explanation for the acanthosis. IL6 is a keratinocyte mitogen (Werner et al, 2007), and its overexpression may contribute to the hyperproliferation in K5cre-CMVcaNrf2 mice. Furthermore, the keratinocyte mitogens colony stimulating factor 2 (*Csf2*), *Csf3* and hepatocyte growth factor (*Hgf*), which are upregulated by pro-inflammatory cytokines (Szabowski et al, 2000), were expressed at higher levels at P32, but not at P2.5 or 6 months of age (Fig 4C). This time course of expression also reflects the progression and amelioration of the phenotype (see Fig 3A).

Tight junctional permeability is not affected in caNrf2 transgenic mice

The physical barrier of the epidermis is formed by the protein-enriched corneocytes (CO) with their cornified envelope (CE) and by lipid-enriched intercellular domains. In addition, corneodesmosomes as well as tight junctions in the granular layer contribute to the barrier (Proksch et al, 2008). We therefore analysed these components in our mice.

Ultrastructural analysis revealed enlarged intercellular spaces in the granular layer of the epidermis of P32 K5cre-CMVcaNrf2 mice (Fig 5A). However, there was no major difference in the number of desmosomes in the granular layer.

Since tight junctions are important components of the epidermal barrier (Furuse et al, 2002; Yang et al, 2010), we tested their functionality. For this purpose we performed a diffusion assay by intradermal injection of a 600 Da sulfo-NHS-LC-biotin into the tail skin. In control mice, sulfo-NHS-LC-biotin was detected in the intercellular space of keratinocytes up to the upper part of the granular layer, where tight junctions are located that prevent further diffusion (Furuse et al, 2002). A similar distribution was observed in K5cre-CMVcaNrf2 mice, indicating that tight junction permeability is not grossly affected (Fig 5B).

Abnormal epidermal lipid metabolism in K5cre-CMVcaNrf2 mice

To determine if epidermal lipids are affected in K5cre-CMVcaNrf2 mice, we analysed the lamellar bodies (LB), which are lipid packed granules formed in differentiated keratinocytes. Ultrastructural analysis revealed malformed LB in P32 K5cre-CMVcaNrf2 mice with disoriented lamellae and/or a reduction or total loss of lamellae (Fig 5C). The number of LB was increased. This correlated with the severity of LB malformation, indicating an attempt to compensate for their morphological and consequently functional impairment. Free lamellar structures

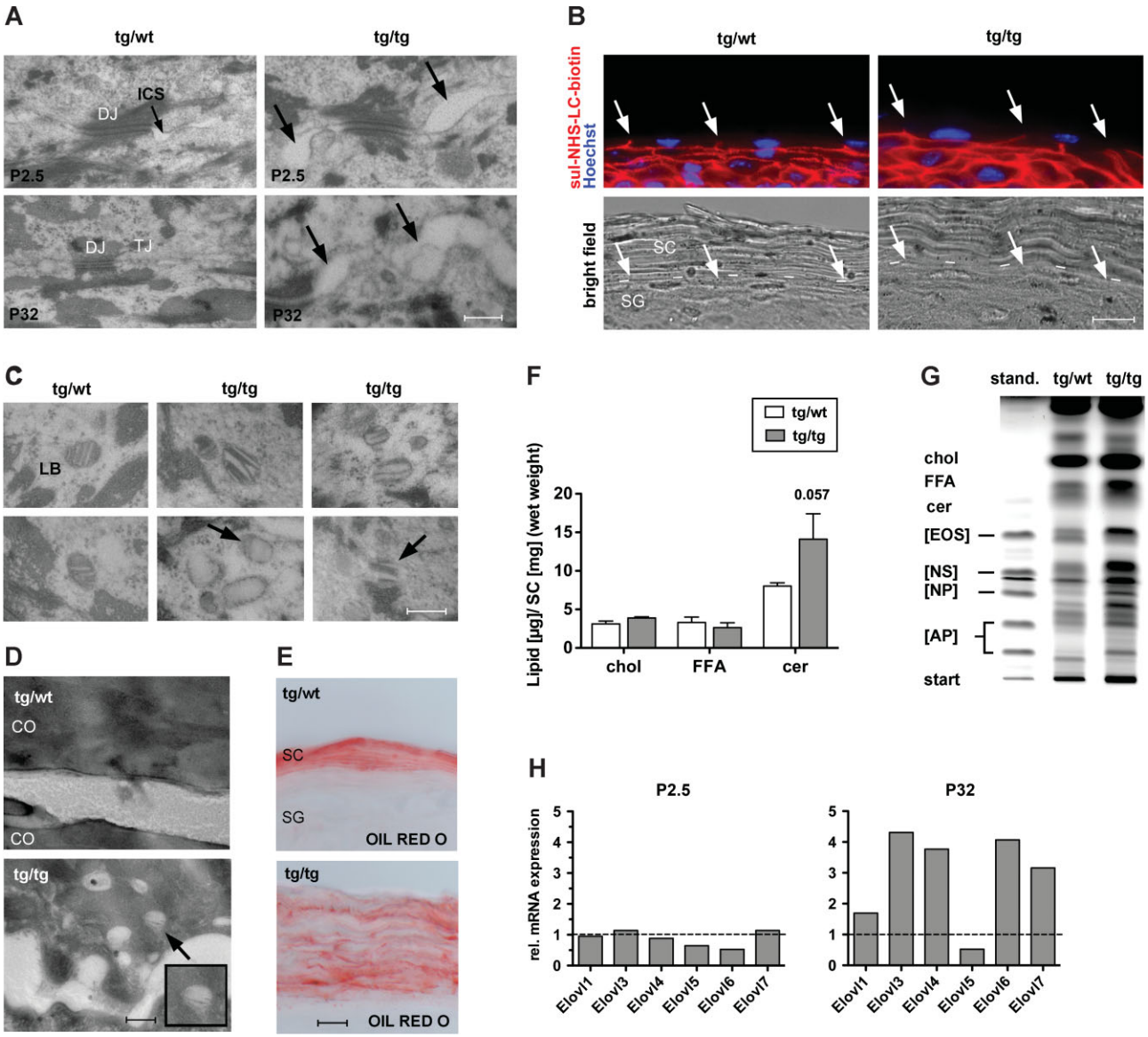

Figure 5. Abnormalities in lamellar bodies and epidermal lipids in K5cre-CMVcaNrf2 mice.

A. Electron microscopy of stratum granulosum (SG) keratinocytes of tg/wt and tg/tg mice at P2.5 and P32. Arrow points to the broadened intercellular space in tg/tg mice. Scale bar: 0.3 μm. DJ, desmosomal junction; TJ, tight junction; ICS, intercellular space.

B. Upper panel: Tight junction permeability assay using sulfo-NHS-LC-Biotin (red), counterstained with Hoechst (blue). Lower panel: Bright field image of the same microscopic field. Arrows point to plasma membranes where diffusion of sulfo-NHS-LC-Biotin is stopped. Dashed line in the lower panel indicates boundary between SG and SC. Scale bar, 10 μm.

C. Electron microscopy of SG keratinocytes of tg/wt and tg/tg mice. Note the LB abnormalities, including disoriented lamellae, reduction of lamellae, complete loss of lamellae or lamellae without surrounding membrane in keratinocytes of the SG in tg/tg mice (indicated by arrow). Scale bar, 0.2 μm.

D. Electron microscopy of CO of tg/wt and tg/tg mice. Note the presence of lamellar bodies in the CO of tg/tg mice (indicated by arrow). Scale bar, 0.2 μm.

E. Oil Red O staining of the SC. Note staining between SC layers. Scale bar, 10 μm.

F. Amount (in μg) of cholesterol, free fatty acids and ceramides relative to the SC wet weight (in mg).

G. HPTLC analysis of SC lipids. Cer, ceramide; Chol, cholesterol; FFA, free fatty acid. Standard contains the SC ceramides Cer [AP], Cer [NP], Cer [NS] and Cer [EOS], which differ with regard to hydroxylation of sphingoid base and fatty acid residues as well as esterification with another fatty acid (Farwanah et al, 2007).

H. qRT-PCR analysis of *Elovl1*, *Elovl3*, *Elovl4*, *Elovl5*, *Elovl6*, *Elovl7* relative to *Gapdh* using RNAs from skin of P2.5 (left, $N = 2/3$) and P32 (right, $N = 3$) K5cre-CMVcaNrf2 relative to control mice. Expression levels of control mice were arbitrary set to 1, indicated by dashed line.

were found in the cytoplasm of keratinocytes in the granular layer of K5cre-CMVcaNrf2 mice (Fig 5C), and occasionally we observed LB in the cytoplasm of CO (Fig 5D). Thus, LB secretion is also disturbed in K5cre-CMVcaNrf2 mice. Nevertheless, lipid secretion and/or formation of the CE seem to occur as revealed by neutral lipid OIL RED O staining (Fig 5E).

Quantification of SC lipids showed a 76% increase in ceramides relative to the SC weight in caNrf2-transgenic mice, while free fatty acids and cholesterol were similar in mice of both genotypes (Fig 5F). High performance thin layer chromatography (HPTLC) analysis of the SC revealed alterations in the distribution of the different classes of ceramides, indicating a change in ceramide modification, such as, for example hydroxylation, desaturation and/or elongation (Fig 5G).

The length of ω-hydroxy long chain fatty acids is critical for an efficient contribution of ceramides to the barrier (Cameron et al, 2007; Li et al, 2007; Westerberg et al, 2004). Long chain fatty acid elongation is a multistep process, with the rate-limiting initial step being catalysed by long-chain fatty acid elongation factors (Elovls; Guillou et al, 2010). A significant upregulation of *Elovl3*, *4*, *6* and *7* was found in P32 K5cre-CMVcaNrf2 mice (Fig 5H). Since Elovls are predominantly regulated at the transcriptional level (Guillou et al, 2010), their upregulation most likely results in an increase in long chain fatty acids. This could at least in part explain the shift in the ceramide pattern seen in the HPTLC analysis. At P2.5, we could not detect obvious alterations in LB morphology and secretion, and upregulation of Elovls was not yet observed at this age (Fig 5H). Therefore, the alterations in lipid metabolism and LB formation and secretion are obviously not a direct effect of Nrf2 activation, but rather a consequence of other epidermal abnormalities.

Upregulation of *Slpi*, *Sprr2d* and *Sprr2h* in K5cre-CMVcaNrf2 mice

Ultrastructural analysis of the SC of P32 K5cre-CMVcaNrf2 mice revealed CO with a translucent cytoplasm in the lower layers of the SC and a thickening of the CO, especially in the back skin (Fig 6A). A regionally restricted thickening of CO was already observed at P2.5, suggesting that alterations in CO are an early abnormality and potentially a direct consequence of Nrf2 action. Processing of filaggrin (Flg), which is required for keratin bundling and thus flattening of keratinocytes, however, was normal in P32 K5cre-CMVcaNrf2 mice (Fig 6B). Furthermore, we did not find alterations in the expression of *Lor* (Fig 6E). Therefore, we wondered if other components of the CE are differentially expressed at this early stage. To address this question we performed a microarray analysis to compare the gene expression pattern in the skin of P2.5 control and K5cre-CMVcaNrf2 transgenic mice. Analysis of the array data revealed a strong upregulation of various known Nrf2 target genes involved in ROS detoxification and/or glutathione metabolism (Table SI of Supporting information). These data further confirm the usefulness of our transgenic model to study Nrf2 function. Among 80 annotated genes, which were more than twofold regulated in either direction, we only identified six genes, for which a role in CE formation and/or epidermal barrier function had been demonstrated (Table 1). These encode the secretory leukocyte peptidase inhibitor (Slpi), the small proline rich proteins (Sprr) 2d and Sprr2h, keratin 16 (K16), cytochrome P450 family 2 subfamily b polypeptide 19 (Cyp2b19) and peroxisome proliferator activator receptor beta/delta (PPARβ/δ).

K16 is upregulated in sulforaphane treated skin (Kerns et al, 2007), and overexpression of K16 in a transgenic mouse model resulted in hyperkeratosis and barrier disturbance (Presland et al, 2004). However, there was only a transient postnatal upregulation of K16 in K5cre-CMVcaNrf2 transgenic mice as determined by immunofluorescence staining (Fig S1E of Supporting information). A role of PPARβ/δ in cutaneous homeostasis and barrier formation has recently been shown (Man et al, 2008). Cyp2b19 is an arachidonic acid epoxygenase, and the resulting product activates transglutaminase, suggesting a role in CE formation (Ladd et al, 2003). Using quantitative polymerase chain reaction (after reverse transcription) (qRT-PCR) analysis we found only a marginal upregulation of *Cyp2b19* and *PPARβ/δ* expression in P2.5 and P32 K5cre-CMVcaNrf2 transgenic mice (Fig S1F and G of Supporting information). Therefore, a major role of these genes in the development and progression of the skin phenotype of K5cre-CMVcaNrf2 mice seems unlikely.

Slpi was previously identified as an Nrf2 target in alveolar macrophages (Ishii et al, 2005). In the epidermis Slpi inhibits the serine protease kallikrein 7 (Klk7; Franzke et al, 1996), which is involved in SC desquamation by degradation of corneodesmosome proteins (Caubet et al, 2004). Thus, upregulation of Slpi is likely to result in reduced desquamation. Enhanced expression of *Slpi* in P2.5 K5cre-CMVcaNrf2 mice was confirmed by qRT-PCR, and a more than 30-fold increase in expression compared to control mice was seen at this early stage (Fig 6C). *Slpi* expression was already increased at P0.5 (Fig S2A of Supporting information), suggesting that its upregulation in K5cre-CMVcaNrf2 mice is a primary effect of Nrf2 activation. Consistent with the severe hyperkeratosis in adult mice (see Fig 3A), a more than 100-fold increase in *Slpi* mRNA levels was seen at P32 (Fig 6C).

To determine if the *Slpi* upregulation is indeed functionally important, we analysed the corneodesmosomes. In K5cre-CMVcaNrf2 mice corneodesmosomes were indeed still present in the most upper layers of the hyperthickened SC as determined by immunofluorescence staining for desmoplakin (Dpn; Fig S2B of Supporting information). Ultrastructural analysis of the corneodesmosomes in control and K5cre-CMVcaNrf2 mice revealed a delay in corneodesmosome degradation in transgenic mice (Fig 6D). This suggests that the upregulation of Slpi is involved in the hyperkeratosis of caNrf2 transgenic mice by inhibition of the Klk7-mediated degradation of CO and subsequent desquamation.

Sprrs are important components of the CE (Patel et al, 2003), which are cross-linked to Lor during CE formation. The upregulation of *Sprr2d* and *Sprr2h* in P2.5 K5cre-CMVcaNrf2 mice was confirmed by qRT-PCR (Fig 6E). Consistent with the array data, expression of Sprr1a was not regulated. At P0.5, levels of *Sprr2h* and particularly of *Sprr2d* mRNAs were already increased (Fig S2A of Supporting information) demonstrating that their enhanced expression correlates with the early morphological alterations of the CO. Expression of *Sprr2d*

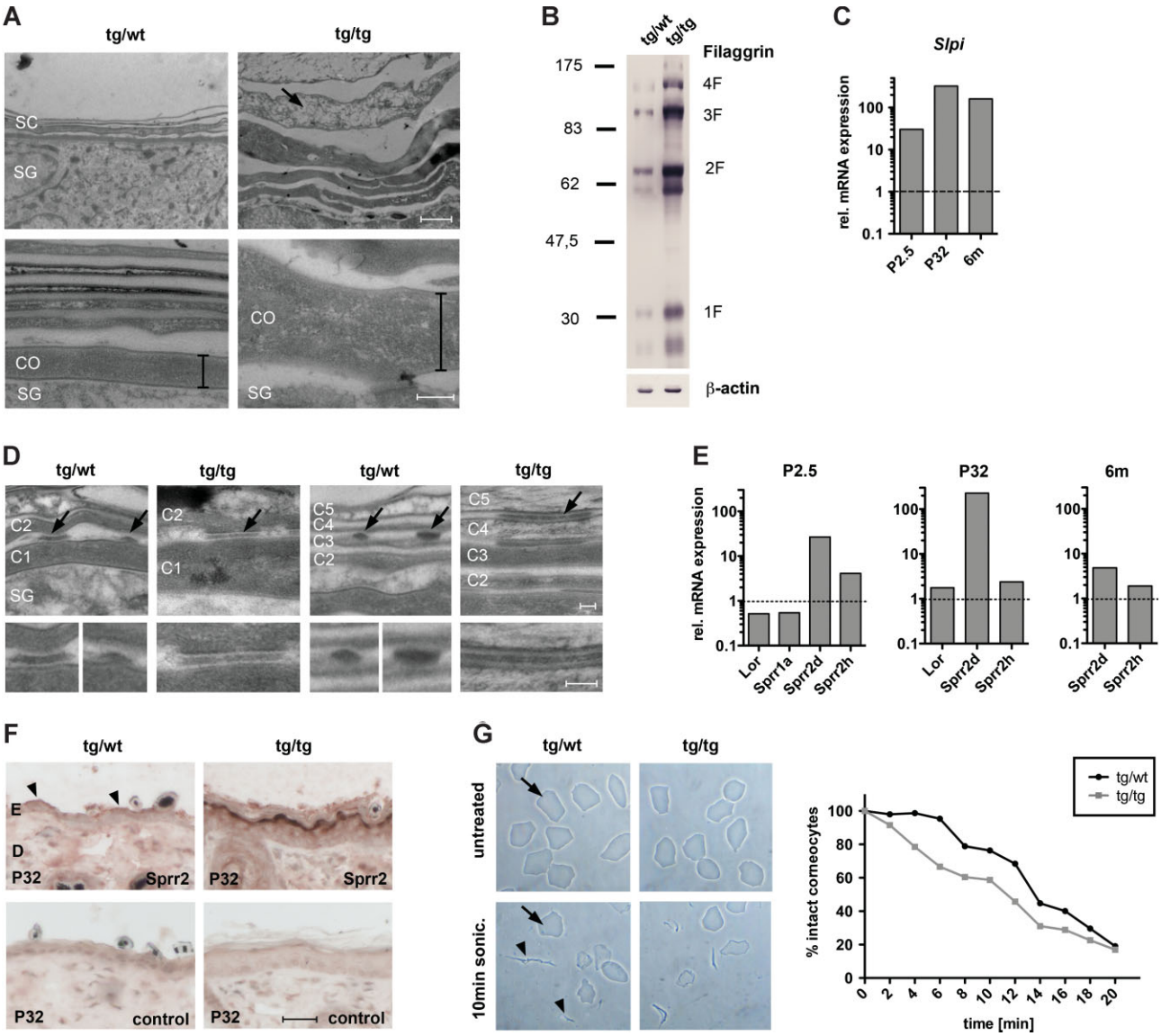

Figure 6. Corneocyte abnormalities and upregulation of *Slpi*, *Sprr2d* and *Sprr2h* in K5cre-CMVcaNrf2 mice.

A. Electron microscopy of the upper epidermis in P32 tg/wt and tg/tg mice. Bar in lower panel indicates thickness of the first corneocyte in the SC connected to the stratum granulosum (SG) in tg/wt and tg/tg mice. Arrow in upper panel of tg/tg mice points to corneocyte with translucent cytoplasm. Scale bars, 1 μm (left panel); 0.2 μm (right panel).

B. Western blot analysis of skin lysates for Flg and β-actin.

C. qRT-PCR of *Slpi* relative to *Gapdh* using skin RNAs from P2.5 ($N = 2/3$), P32 ($N = 3$) and 6 months ($N = 3$) tg/tg and tg/wt mice. Expression levels of control mice were arbitrarily set to 1 (dashed line).

D. Electron microscopy of the lower (left panel) and upper (right panel) SC in P32 tg/wt and tg/tg mice. Corneodesmosomes are indicated by arrows and shown at high magnification in the lower panel. CO are numbered from basal to suprabasal (C1–C5). Note partially degraded corneodesmosomes of lower and upper CO in tg/wt mice, but intact corneodesmosomes in tg/tg mice. Scale bars, 0.1 μm, upper and lower panel.

E. qRT-PCR of *Lor*, *Sprr1a*, *Sprr2d* and *Sprr2h* relative to *Gapdh* using skin RNAs from P2.5 ($N = 2/3$), P32 ($N = 3$) and 6 months ($N = 3$) tg/tg and tg/wt mice.

F. Immunohistochemical staining of tail skin sections with an Sprr2 antibody or without primary antibody (control). Scale bars, 30 μm.

G. Ultrasound treatment of dissociated CO. Upper panel: Representative picture of untreated CO (top) and of CO after 10 min of sonication (bottom). Arrows point to intact CO, arrowheads to cell debris of damaged CO. Graph: Percentage of intact CO after 2–20 min of sonication relative to untreated CO. Note faster destruction of tg/tg compared to tg/wt CO.

further increased in transgenic mice at P32, but declined again in 6-month-old mice (Fig 6E). This correlates with the strong phenotype and increase in TEWL at P32 (Fig 3A, F). *Sprr2h*, in contrast, was already downregulated at P32 (Fig 6E). A strong increase in the expression of Sprr2s in P32 K5cre-CMVcaNrf2 was also observed by immunohistochemistry using an antibody that detects multiple Sprr2 variants (Fig 6F).

We next investigated whether the upregulation of Sprrs in caNrf2 transgenic mice impairs the mechanical stability of the CO. We therefore isolated these cells from back skin of P2.5 mice and subjected them to ultrasound treatment (Koch et al, 2000). Dissociated CO of K5cre-CMVcaNrf2 mice appeared morphologically normal, but ultrasound treatment resulted in a faster destruction of CO from caNrf2-expressing mice compared to control animals (Fig 6G). This was also observed for CO from the tail of P32 K5cre-CMVcaNrf2 mice (Fig S2C of Supporting information).

Slpi, *Sprr2d* and *Sprr2h* are novel Nrf2 targets in keratinocytes

Finally we investigated the mechanism of *Slpi*, *Sprr2d* and *Sprr2h* regulation by Nrf2. Upon topical administration of *t*BHQ or sulforaphane to WT mice we observed upregulation of *Slpi* and *Sprr2d*, but not of *Sprr2h* and *Lor* (Fig 7A and Fig S2D of Supporting information). Enhanced expression of *Slpi* and *Sprr2d* was also observed in primary keratinocytes isolated from P4 K5cre-CMVcaNrf2 mice (Fig 7B).

When primary keratinocytes from WT mice were treated with *t*BHQ, we found a strong upregulation of *Slpi*, *Sprr2d* and *Sprr2h* (Fig 7C). The increase in *Sprr2d* and *Sprr2h* expression was in a similar range as the upregulation of the established Nrf2 target *Nqo1*, and the upregulation of *Slpi* was only slightly lower (Fig S2E of Supporting information). Most importantly, the increase in *Slpi*, *Sprr2d* and *Nqo1* expression was not observed upon *t*BHQ treatment of keratinocytes from *Nrf2* ko mice (Fig 7C

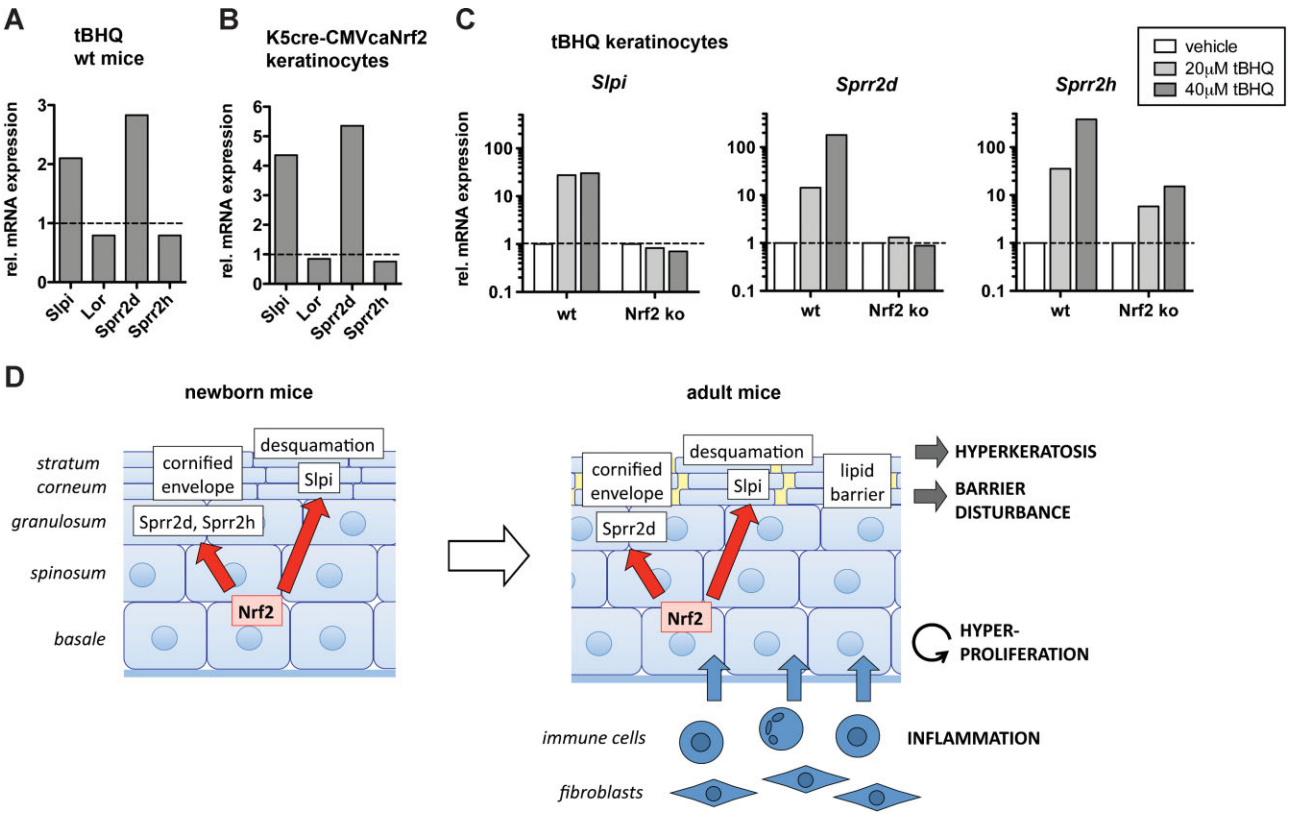

Figure 7. Regulation of *Slpi*, *Sprr2d* and *Sprr2h* by Nrf2.

A,B. qRT-PCR of *Slpi*, *Lor*, *Sprr2d* and *Sprr2h* relative to *Gapdh* using RNAs from P10 *t*BHQ-creamed ($N = 3$) and vehicle-creamed ($N = 3$) wt mice (**A**) and from primary keratinocytes of tg/tg and tg/wt mice (**B**).

C. qRT-PCR of *Slpi*, *Sprr2d* and *Sprr2h* relative to *Gapdh* using RNAs from primary keratinocytes of WT and *Nrf2* ko mice treated with vehicle or *t*BHQ as indicated.

D. Model of Nrf2 action in the epidermis of K5cre-CMVcaNrf2 mice. Left: Nrf2 activation initially leads to an increase in *Slpi*, *Sprr2d* and *Sprr2h* expression. Slpi upregulation reduces desquamation by inhibition of Klk7. Sprr2d and Sprr2h upregulation causes alterations in the composition of the CE. Right: In adult mice inhibition of desquamation causes severe hyperkeratosis. The change in the CE composition results in corneocyte fragility and consequent cracks in the SC. Furthermore, LB abnormalities, defects in their secretion and changes in lipid metabolism occur. These alterations impair the permeability barrier, resulting in skin dryness and initiation of an inflammatory response with subsequent production of pro-inflammatory cytokines and keratinocyte mitogens. Cytokines are involved in alterations of lipid metabolism. Keratinocyte mitogens produced by inflammatory cells and/or fibroblasts cause hyperproliferation of keratinocytes, leading to acanthosis and acceleration of the hyperkeratosis.

and Fig S2E of Supporting information). *Sprr2h* upregulation was reduced upon loss of Nrf2, although not completely abolished (Fig 7C). These findings indicate that *Slpi*, *Sprr2d* and *Sprr2h* are direct targets of Nrf2 and that their upregulation in K5cre-CMVcaNrf2 mice is not the consequence of other epidermal abnormalities.

In K14dnNrf2 transgenic mice, in which Nrf signalling is blocked in keratinocytes by expression of a dominant-negative mutant (auf dem Keller et al, 2006), there was no downregulation of *Slpi*, *Sprr2d* and *Sprr2h* (Fig S2F of Supporting information). Therefore, the basal Nrf2 activity is obviously not sufficient for *Slpi*, *Sprr2d* and *Sprr2h* regulation. Rather, activated Nrf2 is required for their regulation under stress conditions.

DISCUSSION

Genetic and pharmacological activation of Nrf2 in the skin causes ichthyosis-like abnormalities

Pharmacological activation of Nrf2 is a promising approach for the prevention and/or therapy of major human diseases. In the skin, Nrf2 activators protected the epidermis from UV-induced cell damage (Dinkova-Kostova et al, 2006) and ameliorated the blistering in a mouse model of epidermolysis bullosa simplex (Kerns et al, 2007). However, it may also have undesired effects as suggested by the phenotype of *Keap1* ko mice (Wakabayashi et al, 2003).

Here, we show that genetic or pharmacological Nrf2 activation causes severe skin abnormalities, which resemble those of ichthyosis patients (Hohl & Williams, 2011). Therefore, the dosage and duration of a topical treatment with Nrf2 activators needs to be determined for each compound and indication. In addition, it would be important to identify compounds that selectively induce the protective response but not the epidermal abnormalities. This requires a thorough understanding of the mechanisms underlying the Nrf2-induced acanthosis and hyperkeratosis. In this study we addressed these mechanisms and we identified novel and unexpected activities of Nrf2 in CE and epidermal barrier formation. These results reveal that multiple epidermal defense mechanisms are tightly linked through Nrf2.

Nrf2 activation causes keratinocyte hyperproliferation and acanthosis

The availability of a viable mouse model with an Nrf2 gain-of-function allowed us to address the mechanisms underlying the epidermal phenotype. We found that the severe acanthosis resulted predominantly from an increase in keratinocyte proliferation. Although activated Nrf2 enhanced the proliferation of certain tumour cells *in vitro* (Homma et al, 2009; Reddy et al, 2008), this was not the case for cultured keratinocytes from caNrf2 transgenic mice. Rather, the hyperproliferation seen *in vivo* is most likely a consequence of a disturbed epidermal barrier as seen in other mouse lines with barrier defects (Djalilian et al, 2006; Yang et al, 2010), in WT mice after acute barrier disruption (Wood et al, 1992), and in patients suffering from diseases with an impaired epidermal barrier, such as psoriasis, atopic dermatitis and ichthyoses (Elias et al, 2008; Proksch et al, 2008; Wagner et al, 2010). These conditions are also characterized by cutaneous inflammation.

K5cre-CMVcaNrf2 mice showed an increase in the number of mast cells, T-cells and neutrophils and enhanced expression of several pro-inflammatory cytokines at P32. At P2.5, no change in immune cell number and only a slight upregulation of *Il1β* was observed. This correlates with the onset of the barrier defect, which was first detected at P10. Thus, the inflammation is most likely the consequence of the barrier defect. Activated immune cells frequently produce keratinocyte mitogens or induce their production by adjacent fibroblasts (Werner et al, 2007). This was also observed in K5cre-CMVcaNrf2 mice, indicating that caNrf2 affects keratinocyte proliferation through induction of a paracrine loop involving inflammatory cells and possibly mesenchymal cells of the dermis (Fig 7D). This provides a likely explanation for the acanthosis and may also contribute to the hyperkeratosis.

The phenotype of K5cre-CMVcaNrf2 mice is most similar to the abnormalities seen in patients with lamellar ichthyosis. This is based on three histological criteria: An acanthotic epidermis with 4–7 malpighian layers, a massive hyperorthokeratosis lacking histological atypia, and a mild erythema with only a slight increase in mononuclear infiltrate and moderate increase in mast cells and neutrophils (Fig S3 of Supporting information). However, a direct comparison of the mouse phenotype with the human disease is limited by the anatomical differences between murine and human skin.

Activation of Nrf2 interferes with corneocyte desquamation

The major reason for the severe hyperkeratosis in caNrf2 transgenic mice is most likely the upregulation of Slpi. It was previously shown that Slpi inhibits Klk7 (Franzke et al, 1996), which is involved in the desquamation of the SC by degradation of corneodesmosomes (Borgono et al, 2007; Caubet et al, 2004).

Table 1. Genes involved in epidermal barrier formation with ≥2-fold change ($p < 0.005$) in microarray using back skin RNA of P2.5 K5cre-CMVcaNrf2 and control mice.

Symbol	Gene name	Fold Change	Reference
Slpi	Secretory leukocyte peptidase inhibitor	6.3	Caubet et al (2004)
Sprr2d	Small proline-rich protein 2D	5.2	Patel et al (2003)
Sprr2h	Small proline-rich protein 2H	3.2	Patel et al (2003)
Krt16	Keratin 16	3.1	Presland et al (2004)
Cyp2b19	Cytochrome P450 family 2 subfamily b polypeptide 19	2.0	Ladd et al (2003)
Pparβ/δ	Peroxisome proliferator activator receptor beta/delta	2.0	Man et al (2008)

We showed by ultrastructural analysis that corneodesmosome degradation is indeed delayed in K5cre-CMVcaNrf2 mice. Thus, the strong upregulation of Slpi in K5cre-CMVcaNrf2 mice is likely to impair corneodesmosome degradation by inhibition of Klk7, resulting in delayed desquamation. This is the likely mechanism underlying the severe hyperkeratosis in these mice.

Regulation of *Slpi* by Nrf2 had previously been shown in alveolar macrophages, and Slpi was identified as a direct target of Nrf2 using reporter assays. Nrf-mediated upregulation of Slpi and the resulting inhibition of elastase activity contributed to the anti-inflammatory and protective function of Nrf2 in pulmonary diseases (Ishii et al, 2005). Furthermore, an antimicrobial function of Slpi against fungi and bacteria and an antioxidant function had been demonstrated (Doumas et al, 2005; Wiesner & Vilcinskas, 2010). The identification of *Slpi* as a target of Nrf2 in keratinocytes (this study) therefore suggests that it may contribute to an anti-inflammatory, antimicrobial and antioxidant function of Nrf2 in the epidermis.

Activation of Nrf2 results in cornified envelope instability and consequent barrier disturbance

While the upregulation of Slpi provides a likely explanation for the hyperkeratosis in K5cre-CMVcaNrf2 mice, it does not explain the barrier function defect. Barrier abnormalities may result from alterations in lipid metabolism and LB formation/secretion (Elias et al, 2008) or from defective tight junctions (Hadj-Rabia et al, 2004). The latter possibility was excluded, since the tight junctional permeability was obviously not affected. By contrast, we found a severely altered morphology of LB and disturbed LB secretion. Abnormalities in LB were seen in mouse models of ichthyoses resulting from mutations in genes involved in lipid metabolism (Elias et al, 2008). Indeed, the levels of ceramides were elevated and the ceramide composition was altered in the SC of K5cre-CMVcaNrf2 mice. This is likely to result from enhanced expression of different *Elovls* and a consequent increase in long chain fatty acids. Interestingly, mice lacking *Elovl3* or *Elovl4* show a compromised epidermal barrier due to altered lipid composition (Vasireddy et al, 2007; Westerberg et al, 2004). In the future it will be interesting to study whether overexpression of these genes impairs or improves the epidermal barrier. The increase in ceramides could also be the consequence of elevated cytokine expression, since TNF signalling activated sphingomyelinase in keratinocytes (Jensen et al, 1999). Independent of the underlying mechanism, the lipid abnormalities were obviously not a direct consequence of Nrf2 activation, since they occurred rather late during postembryonic development. Rather, our ultrastructural data revealed early abnormalities in the CE. Expression of *Flg*, which is mutated in a large percentage of patients with ichthyosis vulgaris or atopic dermatitis (Sandilands et al, 2009), was enhanced in adult K5cre-CMVcaNrf2 mice, but the protein was normally processed. Furthermore, upregulation of *Flg* mRNA was not yet observed at P2.5 (microarray data). However, an early and strong upregulation of *Sprr2d* and *Sprr2h* occurred, while expression of *Lor* was unaltered. Sprr2 proteins are cross-linked to Lor by transglutaminase and form an integral part of the CE. In *Lor* ko mice a change in the mechanical stability of the CO had been shown (Koch et al, 2000), which was similar to the defect observed in K5cre-CMVcaNrf2 mice. Thus, the increase in Sprr2d and Sprr2h expression and the consequent abnormal composition of the CE may well be responsible for the CO fragility. Consistent with this assumption, epidermal barrier disturbances were observed in several mouse models with defects in CE proteins (Scharschmidt et al, 2009; Sevilla et al, 2007), and mutated *Sprr3* was recently identified as a risk factor for atopic dermatitis (Marenholz et al, 2011). Thus, the early upregulation of *Sprr2* genes and consequent CE abnormalities are likely to represent the primary defect in K5cre-CMVcaNrf2 mice.

Altered morphology and disturbed secretion of LB were seen in mice with a frameshift mutation in the *Flg* gene that mimics some mutations found in atopic dermatitis patients (Scharschmidt et al, 2009). This finding suggests that defects in the CE also affect LB secretion and thus the composition of the extracellular matrix that normally forms the permeability barrier. This model implies that the defects in lipid metabolism are secondary to the CE abnormalities, a hypothesis that is supported by the time course of events that we observed in our transgenic mice. The resulting barrier defect causes skin dryness and initiates an inflammatory response, which is likely to further impair epidermal lipid metabolism (Jensen et al, 1999; Watson et al, 2007).

Sprrs are novel Nrf2 target genes that contribute to its ROS-protective effect

The present study provides first evidence for a direct regulation of *Sprr2d* and *Sprr2h* genes by Nrf2. This conclusion is based on their early upregulation in newborn skin of K5cre-CMVcaNrf2 mice and on the *t*BHQ-mediated upregulation in keratinocytes from WT but not from *Nrf2* ko mice. Furthermore, classical Nrf2 binding sites (antioxidant response element; ARE; Rushmore et al, 1991) are present in the promoter regions of *Sprr2d* and *Sprr2h* (data not shown). The identification of *Sprr2s* as novel Nrf2 targets provides further insight into the mechanisms underlying the potent ROS-protective effect of Nrf2 in the epidermis, since Sprrs are major ROS-scavengers (Vermeij et al, 2011). Unfortunately, however, chronic deregulated expression postnatally, in particular of Sprr2d, also resulted in an adverse event, the development of an ichthyosis-like skin disease. This undesired activity limits the use of Nrf2 activators for skin protection under stress conditions.

MATERIALS AND METHODS

Generation of caNrf2 transgenic mice

A vector allowing Cre-mediated expression of caNrf2 (Schäfer et al, 2010) was modified by cloning of a *CMV* enhancer in front of the β-actin promoter (Sawicki et al, 1998). Transgenic mice were generated by pro-nucleus injection (FVB/N background). Genotyping of founder mice was performed by PCR (Schäfer et al, 2010) using CMVcaNrf2 primers (Table II of Supporting information).

Microarray analysis

Skin from female P2.5 K5cre-CMVcaNrf2 and control mice was removed and snap frozen in liquid nitrogen. RNA purification, reverse

The paper explained

PROBLEM:

The skin, which serves as a protective barrier against the environment, is frequently challenged by harmful insults that cause formation of reactive oxygen species (ROS). A central player in the ROS defense is the transcription factor Nrf2, a promising pharmacological target for skin protection and cancer prevention. The consequences of long-term activation of Nrf2 in the skin, however, are poorly understood. In addition, it was previously unclear if Nrf2 also controls other components of the epidermal barrier.

RESULTS:

We show that genetic or pharmacological activation of Nrf2 in murine keratinocytes induced epidermal thickening and hyperkeratosis resembling the human skin disease lamellar ichthyosis. The discovery of three novel Nrf2 targets in keratinocytes provides a mechanistic explanation for the phenotype: While upregulation of the secretory leukocyte peptidase inhibitor (Slpi) caused hyperkeratosis through inhibition of desquamation, Nrf2-mediated expression of small proline-rich proteins (Sprr2) d and h resulted in corneocyte fragility with a concomitant defect in epidermal barrier function and development of inflammatory skin disease. Activation of the Nrf2-Sprr2 and Nrf2-Slpi pathways enhances the epidermal antioxidant and antimicrobial defense, but prolonged and enhanced activation causes corneocyte fragility and alterations in the epidermal barrier.

IMPACT:

The results described in this study identify Nrf2 as a central regulator of various protective functions of the epidermis. While these activities are generally beneficial, prolonged and enhanced activation of these pathways is detrimental and limits the therapeutic potential of Nrf2 activators.

transcription, labelling, microarray hybridization and analysis were performed as described earlier (Beyer et al, 2008). Microarray analysis was performed using RNAs from three individual mice per genotype. The microarray data have been deposited in NCBI's Gene Expression Omnibus (Edgar et al, 2002) and are accessible through GEO Series accession number GSE35160 (http://www.ncbi.nlm.nih.gov/geo/query/acc.cgi?acc=GSE35160).

Topical treatment of mice with Nrf2 activators

Mice were treated twice a day for 10 consecutive days starting at P0 with a 1:2 mixture of non-ionic hydrophilic cream (Hänseler, Herisau, Switzerland) and DMSO (vehicle) supplemented with 10 mM sulforaphane or 50 mM *t*BHQ (both from Merck, Darmstadt, Germany) and sacrificed by CO_2 inhalation. All animal experiments had been approved by the local veterinary authorities of Zurich, Switzerland (Kantonales Veterinäramt Zürich).

Morphometric analyses

Epidermal thickness was analysed by measurement of the interfollicular epidermal area and corresponding length on H&E stained longitudinal paraffin sections (7 μm) from mouse back skin. Morphometrical analyses were performed using the Openlab 3.1.5 software (Perkin Elmer, Waltham, MA).

Analysis of TEWL

TEWL was analysed on shaved posterior back skin of anesthetized mice using a Tewameter (Courage and Khazaka Electronic GmbH, Cologne, Germany). 50 consecutive and three independent measurements were performed according to the manufacturer's instructions.

Tight junction permeability assay

20–30 μl of EZ-Link™ Sulfo-NHS-LC-Biotin solution (Pierce Chemical Co.; 10 mg/ml in 1 μM $CaCl_2$/PBS) were intradermally injected into the tail skin of anesthetized adult mice. Mice were sacrificed 1 h after injection and sulfo-NHS-LC-Biotin was detected on 7 μm cryosections (Furuse et al, 2002).

Isolation of corneocytes and ultrasound treatment

CO were isolated (Koch et al, 2000) and counted in a Neubauer chamber. Equal amounts of CO from K5cre-CMVcaNrf2 and control mice were suspended in the same volume and sonicated for 20 min in a Branson 2510 cup sonicator (Branson Ultrasonics, Danbury, CT) at 4°C. Every 2 min an aliquot was taken and the number of intact CO was counted.

Lipid extraction and HPTLC

The SC was manually separated after 3 h incubation of tail skin in 0.5% trypsin in PBS at 37°C and 30 min sonication. Lipids were extracted from SC using chloroform/methanol and water (2:1:0.8 by volume). After a phase separation step the lower chloroform phase was used for further analysis. Separation of the lipids on silica HPTLC plates was performed using a solvent mixture consisting of *n*-hexane, diethyl ether and acetic acid (70:30:1 by volume). A second chromatography step (to the top of the plate) using chloroform, methanol and acetic acid (190:9:1 by volume) allowed the separation of ceramides. Extractions of samples from tg/wt and tg/tg mice were performed simultaneously.
The separated lipid bands were visualized by dipping the plates into an aqueous solution containing 10% $CuSO_4$, 8% H_3PO_4 (w/v) and subsequent heating to 160°C for 10 min. Thereafter, the visualized lipid bands were scanned densitometrically in the reflectance mode at a wavelength of 595 nm using a TLC Scanner 3 (CAMAG, Berlin, Germany). Quantitative results were obtained by relating the intensities of the separated lipid bands to calibration curves of corresponding standards.

Replicate experiments and statistical analyses

For qRT-PCR and Western blot analyses, either single animals or pools of skin samples from 2 to 3 mice from one litter or pools of 2 to 3

dishes of cells were used, and all experiments were repeated with independent samples. BrdU analyses were performed in triplicates. Statistical analyses were performed using the non-parametric Mann–Whitney *U*-test for non-Gaussian distribution and Prism 5.0 software (GraphPad Software, La Jolla, CA). Error bars represent standard deviation.

For more detailed Materials and Methods see the Supporting information. Primers are listed in Table SII, antibodies in Table SIII of Supporting information.

Author contributions

MS performed experiments, designed experiments together with SW and wrote the manuscript together with SW; HF, AHW, AJH and WB performed experiments and analysed the data; KS and DR contributed to the design of experiments and data analysis; DH provided samples and pictures from patients with lamellar ichthyosis and helped with the histological comparison of the mouse phenotype with human ichthyosis; SW designed the study and the experiments together with MS and wrote the manuscript together with MS.

Acknowledgements

We thank Nicole Hallschmid, Christiane Born-Berclaz, Heike Hupfer and Klaudia Brysch for excellent technical assistance, Gabriele Fenini, Jörg Renkawitz, Sabine Dütsch and Lola Kappeler for help with the characterization of the transgenic mice, Dr. Stefan Zoller, Catharine Aquino and Dr. Hubert Rehrauer (Functional Genomics Center Zurich) for help with the microarray experiments, Dr. José L. Jorcano (CIEMAT, Madrid, Spain) for K5Cre mice, Dr. Yuet Wai Kan (University of California, San Francisco, USA) for Nrf2 ko mice and Dr. Pierre Coulombe (John Hopkins University, Baltimore, USA) for the K16 antibody. This work was supported by the Swiss National Science Foundation (grants 3100A0-109340 and 310030_132884/1 to SW), the Promedica Foundation, Chur, Switzerland (to SW), the CE.R.I.E.S. Award (to SW), the Wilhelm Sander-Stiftung (to SW) and the German Research Foundation (DFG; Sonderforschungsbereich 645, to KS). MS was supported by an EMBO postdoctoral fellowship.

Supporting information is available at EMBO Molecular Medicine online.

The authors declare that they have no conflict of interest.

References

auf dem Keller U, Huber M, Beyer TA, Kumin A, Siemes C, Braun S, Bugnon P, Mitropoulos V, Johnson DA, Johnson JA, *et al* (2006) Nrf transcription factors in keratinocytes are essential for skin tumor prevention but not for wound healing. Mol Cell Biol 26: 3773-3784

Beyer TA, Xu W, Teupser D, auf dem Keller U, Bugnon P, Hildt E, Thiery J, Kan YW, Werner S (2008) Impaired liver regeneration in Nrf2 knockout mice: role of ROS-mediated insulin/IGF-1 resistance. EMBO J 27: 212-223

Bishop NA, Guarente L (2007) Two neurons mediate diet-restriction-induced longevity in *C. elegans*. Nature 447: 545-549

Borgono CA, Michael IP, Komatsu N, Jayakumar A, Kapadia R, Clayman GL, Sotiropoulou G, Diamandis EP (2007) A potential role for multiple tissue kallikrein serine proteases in epidermal desquamation. J Biol Chem 282: 3640-3652

Cameron DJ, Tong Z, Yang Z, Kaminoh J, Kamiyah S, Chen H, Zeng J, Chen Y, Luo L, Zhang K (2007) Essential role of Elovl4 in very long chain fatty acid synthesis, skin permeability barrier function, and neonatal survival. Int J Biol Sci 3: 111-119

Caubet C, Jonca N, Brattsand M, Guerrin M, Bernard D, Schmidt R, Egelrud T, Simon M, Serre G (2004) Degradation of corneodesmosome proteins by two serine proteases of the kallikrein family, SCTE/KLK5/hK5 and SCCE/KLK7/hK7. J Invest Dermatol 122: 1235-1244

Copple IM, Goldring CE, Kitteringham NR, Park BK (2008) The Nrf2-Keap1 defence pathway: role in protection against drug-induced toxicity. Toxicology 246: 24-33

de Vries HE, Witte M, Hondius D, Rozemuller AJ, Drukarch B, Hoozemans J, van Horssen J (2008) Nrf2-induced antioxidant protection: A promising target to counteract ROS-mediated damage in neurodegenerative disease? Free Radic Biol Med 45: 1375-1383

Demehri S, Morimoto M, Holtzman MJ, Kopan R (2009) Skin-derived TSLP triggers progression from epidermal-barrier defects to asthma. PLoS Biol 7: e1000067

Denicola GM, Karreth FA, Humpton TJ, Gopinathan A, Wei C, Frese K, Mangal D, Yu KH, Yeo CJ, Calhoun ES, *et al* (2011) Oncogene-induced Nrf2 transcription promotes ROS detoxification and tumorigenesis. Nature 475: 106-109

Dinkova-Kostova AT, Jenkins SN, Fahey JW, Ye L, Wehage SL, Liby KT, Stephenson KK, Wade KL, Talalay P (2006) Protection against UV-light-induced skin carcinogenesis in SKH-1 high-risk mice by sulforaphane-containing broccoli sprout extracts. Cancer Lett 240: 243-252

Djalilian AR, McGaughey D, Patel S, Seo EY, Yang C, Cheng J, Tomic M, Sinha S, Ishida-Yamamoto A, Segre JA (2006) Connexin 26 regulates epidermal barrier and wound remodeling and promotes psoriasiform response. J Clin Invest 116: 1243-1253

Doumas S, Kolokotronis A, Stefanopoulos P (2005) Anti-inflammatory and antimicrobial roles of secretory leukocyte protease inhibitor. Infect Immun 73: 1271-1274

Edgar R, Domrachev M, Lash AE (2002) Gene Expression Omnibus: NCBI gene expression and hybridization array data repository. Nucleic Acids Res 30: 207-210

Elias PM (2010) Therapeutic implications of a barrier-based pathogenesis of atopic dermatitis. Ann Dermatol 22: 245-254

Elias PM, Williams ML, Holleran WM, Jiang YJ, Schmuth M (2008) Pathogenesis of permeability barrier abnormalities in the ichthyoses: inherited disorders of lipid metabolism. J Lipid Res 49: 697-714

Farwanah H, Pierstorff B, Schmelzer CE, Raith K, Neubert RH, Kolter T, Sandhoff K (2007) Separation and mass spectrometric characterization of covalently bound skin ceramides using LC/APCI-MS and Nano-ESI-MS/MS. J Chromatogr B Analyt Technol Biomed Life Sci 852: 562-570

Franzke CW, Baici A, Bartels J, Christophers E, Wiedow O (1996) Antileukoprotease inhibits stratum corneum chymotryptic enzyme. Evidence for a regulative function in desquamation. J Biol Chem 271: 21886-21890

Furuse M, Hata M, Furuse K, Yoshida Y, Haratake A, Sugitani Y, Noda T, Kubo A, Tsukita S (2002) Claudin-based tight junctions are crucial for the mammalian epidermal barrier: a lesson from claudin-1-deficient mice. J Cell Biol 156: 1099-1111

Guillou H, Zadravec D, Martin PG, Jacobsson A (2010) The key roles of elongases and desaturases in mammalian fatty acid metabolism: insights from transgenic mice. Prog Lipid Res 49: 186-199

Hadj-Rabia S, Baala L, Vabres P, Hamel-Teillac D, Jacquemin E, Fabre M, Lyonnet S, De Prost Y, Munnich A, Hadchouel M, *et al* (2004) Claudin-1 gene

mutations in neonatal sclerosing cholangitis associated with ichthyosis: a tight junction disease. Gastroenterology 127: 1386-1390

Hayes JD, McMahon M (2009) NRF2 and KEAP1 mutations: permanent activation of an adaptive response in cancer. Trends Biochem Sci 34: 176-188

Hohl D, Williams M (2011) Mendelian disorders of cornification (MEDOC): The ichthyoses. In: *Harper's Textbook of Pediatric Dermatology*, Irvine A, Höger P, Yan A (Eds), Oxford, Blackwell Publishing Ltd.: pp 121.001-070

Homma S, Ishii Y, Morishima Y, Yamadori T, Matsuno Y, Haraguchi N, Kikuchi N, Satoh H, Sakamoto T, Hizawa N, *et al* (2009) Nrf2 enhances cell proliferation and resistance to anticancer drugs in human lung cancer. Clin Cancer Res 15: 3423-3432

Ishii Y, Itoh K, Morishima Y, Kimura T, Kiwamoto T, Iizuka T, Hegab AE, Hosoya T, Nomura A, Sakamoto T, *et al* (2005) Transcription factor Nrf2 plays a pivotal role in protection against elastase-induced pulmonary inflammation and emphysema. J Immunol 175: 6968-6975

Jensen JM, Schutze S, Forl M, Kronke M, Proksch E (1999) Roles for tumor necrosis factor receptor p55 and sphingomyelinase in repairing the cutaneous permeability barrier. J Clin Invest 104: 1761-1770

Kerns ML, DePianto D, Dinkova-Kostova AT, Talalay P, Coulombe PA, (2007) Reprogramming of keratin biosynthesis by sulforaphane restores skin integrity in epidermolysis bullosa simplex. Proc Natl Acad Sci USA 104: 14460-14465

Kim YR, Oh JE, Kim MS, Kang MR, Park SW, Han JY, Eom HS, Yoo NJ, Lee SH (2010) Oncogenic NRF2 mutations in squamous cell carcinomas of oesophagus and skin. J Pathol 220: 446-451

Koch PJ, de Viragh PA, Scharer E, Bundman D, Longley MA, Bickenbach J, Kawachi Y, Suga Y, Zhou Z, Huber M, *et al* (2000) Lessons from loricrin-deficient mice: compensatory mechanisms maintaining skin barrier function in the absence of a major cornified envelope protein. J Cell Biol 151: 389-400

Kundu JK, Surh YJ (2010) Nrf2-Keap1 signaling as a potential target for chemoprevention of inflammation-associated carcinogenesis. Pharm Res 27: 999-1013

Kwak MK, Kensler TW (2010) Targeting NRF2 signaling for cancer chemoprevention. Toxicol Appl Pharmacol 244: 66-76

Ladd PA, Du L, Capdevila JH, Mernaugh R, Keeney DS (2003) Epoxyeicosatrienoic acids activate transglutaminases in situ and induce cornification of epidermal keratinocytes. J Biol Chem 278: 35184- 35192

Li W, Sandhoff R, Kono M, Zerfas P, Hoffmann V, Ding BC, Proia RL, Deng CX (2007) Depletion of ceramides with very long chain fatty acids causes defective skin permeability barrier function, and neonatal lethality in ELOVL4 deficient mice. Int J Biol Sci 3: 120-128

Liby KT, Yore MM, Sporn MB (2007) Triterpenoids and rexinoids as multifunctional agents for the prevention and treatment of cancer. Nat Rev Cancer 7: 357-369

Liou GY, Storz P (2010) Reactive oxygen species in cancer. Free Radic Res 44: 479-496

Man MQ, Barish GD, Schmuth M, Crumrine D, Barak Y, Chang S, Jiang Y, Evans RM, Elias PM, Feingold KR (2008) Deficiency of PPARbeta/delta in the epidermis results in defective cutaneous permeability barrier homeostasis and increased inflammation. J Invest Dermatol 128: 370-377

Marenholz I, Rivera VA, Esparza-Gordillo J, Bauerfeind A, Lee-Kirsch MA, Ciechanowicz A, Kurek M, Piskackova T, Macek M, Lee YA (2011) Association screening in the epidermal differentiation complex (EDC) identifies an SPRR3 repeat number variant as a risk factor for eczema. J Invest Dermatol 131: 1644-1649

Patel S, Kartasova T, Segre JA (2003) Mouse Sprr locus: a tandem array of coordinately regulated genes. Mamm Genome 14: 140-148

Perez-Matute P, Zulet MA, Martinez JA (2009) Reactive species and diabetes: counteracting oxidative stress to improve health. Curr Opin Pharmacol 9: 771-779

Presland RB, Coulombe PA, Eckert RL, Mao-Qiang M, Feingold KR, Elias PM (2004) Barrier function in transgenic mice overexpressing K16, involucrin, and filaggrin in the suprabasal epidermis. J Invest Dermatol 123: 603-606

Proksch E, Brandner JM, Jensen JM (2008) The skin: an indispensable barrier. Exp Dermatol 17: 1063-1072

Ramos-Gomez M, Kwak MK, Dolan PM, Itoh K, Yamamoto M, Talalay P, Kensler TW (2001) Sensitivity to carcinogenesis is increased and chemoprotective efficacy of enzyme inducers is lost in nrf2 transcription factor-deficient mice. Proc Natl Acad Sci USA 98: 3410-3415

Reddy NM, Kleeberger SR, Bream JH, Fallon PG, Kensler TW, Yamamoto M, Reddy SP (2008) Genetic disruption of the Nrf2 compromises cell-cycle progression by impairing GSH-induced redox signaling. Oncogene 27: 5821-5832

Rushmore TH, Morton MR, Pickett CB (1991) The antioxidant responsive element. Activation by oxidative stress and identification of the DNA consensus sequence required for functional activity. J Biol Chem 266: 11632-11639

Sandilands A, Sutherland C, Irvine AD, McLean WH (2009) Filaggrin in the frontline: role in skin barrier function and disease. J Cell Sci 122: 1285-1294

Sawicki JA, Morris RJ, Monks B, Sakai K, Miyazaki J (1998) A composite CMV-IE enhancer/beta-actin promoter is ubiquitously expressed in mouse cutaneous epithelium. Exp Cell Res 244: 367-369

Schäfer M, Dütsch S, auf dem Keller U, Navid F, Schwarz A, Johnson DA, Johnson JA, Werner S (2010) Nrf2 establishes a glutathione-mediated gradient of UVB cytoprotection in the epidermis. Genes Dev 24: 1045-1058

Scharschmidt TC, Man MQ, Hatano Y, Crumrine D, Gunathilake R, Sundberg JP, Silva KA, Mauro TM, Hupe M, Cho S, *et al* (2009) Filaggrin deficiency confers a paracellular barrier abnormality that reduces inflammatory thresholds to irritants and haptens. J Allergy Clin Immunol 124: 496-506 e491–496

Sevilla LM, Nachat R, Groot KR, Klement JF, Uitto J, Djian P, Maatta A, Watt FM (2007) Mice deficient in involucrin, envoplakin, and periplakin have a defective epidermal barrier. J Cell Biol 179: 1599-1612

Sykiotis GP, Bohmann D (2010) Stress-activated cap'n'collar transcription factors in aging and human disease. Sci Signal 3: re3

Szabowski A, Maas-Szabowski N, Andrecht S, Kolbus A, Schorpp-Kistner M, Fusenig NE, Angel P (2000) c-Jun and JunB antagonistically control cytokine-regulated mesenchymal–epidermal interaction in skin. Cell 103: 745-755

Taguchi K, Maher JM, Suzuki T, Kawatani Y, Motohashi H, Yamamoto M (2010) Genetic analysis of cytoprotective functions supported by graded expression of Keap1. Mol Cell Biol 30: 3016-3026

Vasireddy V, Uchida Y, Salem N, Jr., Kim SY, Mandal MN, Reddy GB, Bodepudi R, Alderson NL, Brown JC, Hama H, *et al* (2007) Loss of functional ELOVL4 depletes very long-chain fatty acids (>or =C28) and the unique omega-*O*-acylceramides in skin leading to neonatal death. Hum Mol Genet 16: 471-482

Vermeij WP, Alia A, Backendorf C (2011) ROS quenching potential of the epidermal cornified cell envelope. J Invest Dermatol 131: 1435-1441

Wagner EF, Schonthaler HB, Guinea-Viniegra J, Tschachler E (2010) Psoriasis: What we have learned from mouse models. Nat Rev Rheumatol 6: 704-714

Wakabayashi N, Itoh K, Wakabayashi J, Motohashi H, Noda S, Takahashi S, Imakado S, Kotsuji T, Otsuka F, Roop DR, *et al* (2003) Keap1-null mutation leads to postnatal lethality due to constitutive Nrf2 activation. Nat Genet 35: 238-245

Watson RE, Poddar R, Walker JM, McGuill I, Hoare LM, Griffiths CE, O'Neill CA (2007) Altered claudin expression is a feature of chronic plaque psoriasis. J Pathol 212: 450-458

Werner S, Krieg T, Smola H (2007) Keratinocyte–fibroblast interactions in wound healing. J Invest Dermatol 127: 998-1008

Westerberg R, Tvrdik P, Unden AB, Mansson JE, Norlen L, Jakobsson A, Holleran WH, Elias PM, Asadi A, Flodby P, *et al* (2004) Role for ELOVL3 and fatty acid chain length in development of hair and skin function. J Biol Chem 279: 5621-5629

Wiesner J, Vilcinskas A (2010) Antimicrobial peptides: the ancient arm of the human immune system. Virulence 1: 440-464

Wood LC, Jackson SM, Elias PM, Grunfeld C, Feingold KR (1992) Cutaneous barrier perturbation stimulates cytokine production in the epidermis of mice. J Clin Invest 90: 482-487

Xu C, Huang MT, Shen G, Yuan X, Lin W, Khor TO, Conney AH, Kong AN (2006) Inhibition of 7,12-dimethylbenz(a)anthracene-induced skin tumorigenesis in C57BL/6 mice by sulforaphane is mediated by nuclear factor E2-related factor 2. Cancer Res 66: 8293-8296

Yanaka A, Fahey JW, Fukumoto A, Nakayama M, Inoue S, Zhang S, Tauchi M, Suzuki H, Hyodo I, Yamamoto M (2009) Dietary sulforaphane-rich broccoli sprouts reduce colonization and attenuate gastritis in *Helicobacter pylori*-infected mice and humans. Cancer Prev Res (Phila Pa) 2: 353-360

Yang J, Meyer M, Muller AK, Bohm F, Grose R, Dauwalder T, Verrey F, Kopf M, Partanen J, Bloch W, *et al* (2010) Fibroblast growth factor receptors 1 and 2 in keratinocytes control the epidermal barrier and cutaneous homeostasis. J Cell Biol 188: 935-952

